RSC Advances

PAPER

View Article Online
View Journal | View Issue

Cite this: *RSC Adv.*, 2015, **5**, 4780

Self-assembly of microscopic tablets within polymeric thin films: a possible pathway towards new hybrid materials

Seyed Mohammad Mirkhalaf Valashani,[a] Christopher J. Barrett[b] and Francois Barthelat*[a]

Self-assembly produces materials with highly organized microstructures and attractive properties for a variety of applications. Self-assembly is a process which typically involves molecules or nano-scale objects, with only a few reports of successful self-assembly of objects with larger dimensions (greater than 1 μm). Self-assembly at this length scale is however important, and may find different technological applications because of the possibility to incorporate different functionalities to the building blocks by for example lithographic and microfabrication techniques. Meso-scale self-assembly is also particularly promising to duplicate the structure of natural materials such as nacre (mother of pearl). Here, we fabricated 10 μm sized hexagonal tablets of silicon which self-assembled into a well-packed periodically arranged structure at a water–air interface. The microstructure was secured in a PDMS thin film, which made it stable and more organized compared to the similar large scale assemblies reported in the past. The self-assembled films can serve as building blocks for biomimetic materials, protective coatings, flexible electronics, or tunable optical devices.

Received 24th November 2014
Accepted 10th December 2014

DOI: 10.1039/c4ra15166f

www.rsc.org/advances

1. Introduction

Self-assembly is a process where individual components of a system are autonomously arranged in a designed structure or pattern without human intervention.[1] *In vitro* self-assembly of synthetic materials typically involves molecules and nano-particles, and a large number of such self-assembled molecular or nano-edifices have been reported in the literature.[2,3] Self-assembly is a particularly promising approach because it can produce highly ordered structures, provided that the attraction and repulsion forces between the individual components of the system are well-controlled. To this end, different forces including hydrophobic,[4] magnetic,[5] electrostatic,[6] dipolar,[7] electrophoretic,[8] capillary,[9] and molecular recognition[10] have been utilized to control inter-particle interactions. Procedures such as the Langmuir–Blodgett technique,[11] random ultrasonic agitations,[12,13] droplet evaporation,[14] sedimentation,[15] rotation,[4] mechanical vibration,[16] vibration by sound waves,[17] confinement by liquid crystals,[18] and optical confinement[19] have then been used to assemble particles into ordered structures. Most of these techniques, however, focused on assembling molecules and sub-micrometer particles. In contrast, there are a few reports on successful self-assembly of large objects,[4,20] particularly due to the problems with the stability of the system. In most of the self-assembly processes, attractive surface interactions must overcome the destructive inertia forces (*e.g.* during handling), in order to yield stable materials. A good estimation of the ratio of the surface to the body interactions can be achieved from the surface-to-volume ratio (SA : V).[21] Since SA : V of the molecules/nano-particles is considerably high compared to micron/mm sized particles, they commonly form more stable assemblies. For example, Langmuir–Blodgett monolayer films of molecules, assembled by capillary interactions, can be commonly collected on a solid substrate without any damage to the monolayer, upon dipping the substrate into the solution.[22] The same dipping procedure results in considerable damage to the structure of a self-assembled film of micron-sized particles, attracted by capillary interactions.[13] Assembly of μm- or mm-sized particles therefore requires stronger surface attractions such as polymer binding in order to yield stable structures.[4] Too strong surface interactions such as polyelectrolyte electrostatic attractions, on the other hand, might prevent the relative movement of the particles after coagulation and therefore might interrupt the assembly process.[23] Due to these complications, few successful studies on self-assembly of stable structures made of particles having dimensions larger than 1 μm have been reported.[4] However, self-assembly at this size regime has its own advantages and can find different technological applications including in flexible electrical circuits, modern optical materials, or protective systems.[4,20] Molecules do not yet offer the functionality required for some practical applications such as electrical circuits. On the other hand,

[a]*Department of Mechanical Engineering, McGill University, Montreal, QC, Canada. E-mail: francois.barthelat@mcgill.ca*

[b]*Department of Chemistry, McGill University, Montreal, QC, Canada*

different functionalities such as selective electrical conductivity,[24] magnetism,[25] or hydrophobicity[4] can be incorporated to the particles at μm mm^{-1} scales by for example microfabrication techniques. Also, microfabrication and machining processes can yield particles with variety of shapes in the μm mm^{-1} scales, whereas fabrication of building blocks at nanoscale is mostly restricted to spheres, nanorods, or cubes.[14,15] Meso-scale self-assembly therefore has the potential to overcome some of the main limitations of molecular/nano-scale self-assembly. Microscale periodic structures are also found in natural materials such as nacre (Fig. 1a),[26] natural fibers (Fig. 1b),[27] and diatoms (Fig. 1c),[28] which display unusual and attractive properties.[13,23,29] Duplicating the structure of these sophisticated natural materials also requires innovative fabrication methods, including self-assembly.[30–32] In this study, we focused on self-assembly of ~10 μm sized particles into stable and highly ordered films. Previous attempts to self-assemble similar particles, in terms of size and shape, resulted in films which are less organized and less stable compared to the assemblies reported at the nano-scale.[13,33] The particles interact only through van der Waals, capillary, and electrical double layer forces. Therefore, their arrangement can be easily destroyed upon handling and layer-by-layer assembly. Also, since the shape of the particles used in these studies is irregular and not surface-filling, the assembled layers of particles are not well-packed, leaving them far inferior to the highly organized self-assemblies reported at nano-scale. In this work, we developed a relatively simple approach which addresses the limitations described above. We designed and fabricated hard microscopic tablets with high aspect ratio using microfabrication. With surface functionalization and polymer chemistry, the tablets self-assembled into highly ordered films. The method is scalable and can produce large areas of polymer thin films reinforced with hard tablets, which can be used as a base material for the fabrication of complex three-dimensional microstructures.

2. Self-assembly of aluminum oxide micro-tablets

Microscopic platelets of aluminum oxide have recently become a popular building block for self-assembly and biomimicry studies.[13,35] The size of the tablets made them appropriate choices to explore the assembly conditions for micro-particles with dimensions larger than the particles usually used for self-assembly studies. Therefore, we decided to use these tablets, as a first step, in order to study the effect of different assembly conditions and optimize the process. The tablets we used here were obtained from Antaria limited (WA, Australia) and were ~450 nm thick and 3 to 20 μm in width (Fig. 2a). The objective was to use hydrophobic attractions to drive the assembly process. To this end, the surface of the alumina tablets was functionalized with a hydrophobic self-assembled monolayer of 3-aminopropyltriethoxysilane (APTS), following the method of Bonderer *et al.*[13] (Fig. 2b). 20 ml of APTS was first dissolved in 200 ml of a water–methanol (25 volume% (vol.%) methanol) solution in order to hydrolyze the silane species. 10 g of alumina particles was then added the solution. This

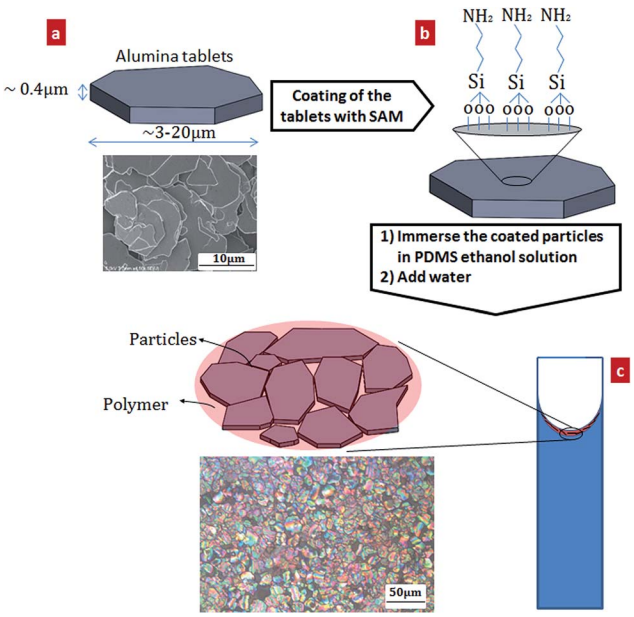

Fig. 2 The self-assembly process. (a) Schematic and a SEM image of alumina tablets. (b) Schematic of an alumina tablet coated with APTS. (c) Schematic of the particles floating at the water–air interface within a polymer thin film, schematic of the self-assembled pack of alumina particles in a PDMS film, and an optical image of the self-assembled particles before the polymer is cured.

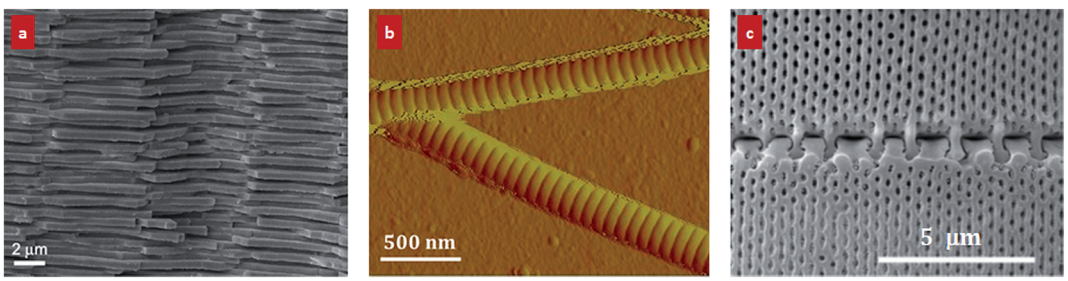

Fig. 1 Intricate periodic structures in (a) Scanning Electron Microscopy (SEM) image of a fracture surface of nacre from a red abalone shell, (b) Atomic Force Microscopy (AFM) image of individual fibrils of collagen type I extracted from a fish scale, (c) surface of the diatom *Ellerbeckia* (adapted from ref. 34).

suspension was then sonicated for 10 min, and stirred for 30 min at 40 °C.[13] The coated particles were then washed by repeated centrifugation/washing with ethanol (4 times), and stored as a stock suspension consisting of pure ethanol with ~4 × 10^5 particles per ml. This stock suspension was used to self-assemble the tablets using the Langmuir–Blodget technique. In order to be able to handle the self-assembled layer of tablets, we also wanted to secure them into a polymeric thin film. Prior to self-assembly, therefore, added to 3 ml of prepared suspension of alumina tablets in a cuvette was 60 μl of a polymer composed of 80/19.8/0.2 vol.% polydimethylsiloxane (PDMS)/tetraethyl orthosilicate (the cross-linker)/dibutyltin dilaurate (the catalyst). After the particles sedimented at the bottom of the cuvette, most of the solution (free of tablets) was removed to keep only about 60 μl of ethanol with polymer and a high concentration of tablets (~2 × 10^7 particles per ml). Water was then slowly added to the cuvette, with two simultaneous effects. Firstly, the presence of water greatly reduced the solubility of the PDMS, which as a result was driven to the hydrophobic surface of the particles (the strategy of lowering the solubility of a solute in a solvent, in order to precipitate it, is often used to purify proteins[36]). In this step, the presence of the hydrophobic APTES layer on the surface of the particles was essential in order to attract the polymer chains. Once precipitated on the surface, a likely mechanism was the amino group of the silane forming hydrogen bonds with the oxygen atoms of the PDMS. Hydrogen bonds can reform reversibly after breaking under loading and therefore can maintain cohesion over large distances and prevent the catastrophic failure of the material. APTS is therefore not only essential in the assembly process; it also promotes interesting deformation/failure mechanisms at the tablet–polymer interface which is encouraging for the future applicability of the films as bio-inspired materials. The second effect of adding water was to aggregate the hydrophobic particles to the water–air interface in order to minimize their interfacial surface energy. The tablets then quickly assembled into islands of approximately 10 to 20 tablets by hydrophobic and capillary attractions.[21] These small particle-reinforced polymer islands were also attracted to each other and assembled by several mechanisms: (i) hydrophobic and possibly capillary attractions, and (ii) gravity which might drive the islands to the bottom of the concave water–air interface in the cuvette (Fig. 2c). Upon coalescence of these islands, a continuous film of particles formed (Fig. 2c).

We identified two main parameters for optimizing the assembly process: (i) the relative concentration of the particles and polymer, and (ii) the amount of catalyst used in the polymer. For optimized assembly conditions, a concentration of ~2 × 10^7 particles per ml was required in a 2 vol.% solution of polymer in ethanol, before adding the water. Having a lower number of particles in the suspension resulted in a sparse population of particles in the polymer thin film (Fig. 3a) while having more particles resulted in disorganized aggregation of particles (Fig. 3b). In the self-assembly process, the polymer chemistry was also crucial. Upon curing, the thin polymeric film shrunk, pulling the tablets closer together, improving their arrangement and also securing them into their final positions. This particular step had to be carefully optimized, because the film of particles typically fractured upon shrinkage, a common problem in the assembly of colloidal crystals.[37] Fig. 3c shows that the film of particles self-assembled using PDMS with high a concentration of catalyst (2 vol.% dibutyltin dilaurate) is extensively cracked during the curing of the polymer. However, we found that cracking could be minimized by reducing the amount of catalyst (to 0.2 vol.%) in the initial polymer mixture, at the expense of increasing the curing time to one week. By optimizing the number of particles and the polymer chemistry in the initial suspension, therefore, thin films of well-packed micron-sized tablets were obtained using this technique (Fig. 4). Since this assembly process is mainly governed by hydrophobic and capillary attractions, it can be categorized as a modified Langmuir–Blodgett technique developed for the assembly of meso-scale sized particles.

Once a well-assembled layer of particles is obtained on the surface of the solution, the particles must be collected for further processing into materials or devices. This can be a challenging step, for which curing the PDMS was crucial. Attempts to collect the tablets from the surface of the solution without using a polymer (a typical procedure used for example in Bonderer *et al.*[13]) or before the polymer is cured inevitably resulted in irreparable damage to the fragile self-assembled patterned structures. Securing the micro-tablets into a thin polymeric film made this procedure more robust, and highly ordered films could be collected on glass slides (Fig. 4a). However, because of the irregular shape of the particles, assembly into periodic patterns is not possible. Also, while the film is about one tablet thick, there is significant overlap and tilting of individual tablets which produce interference fringes

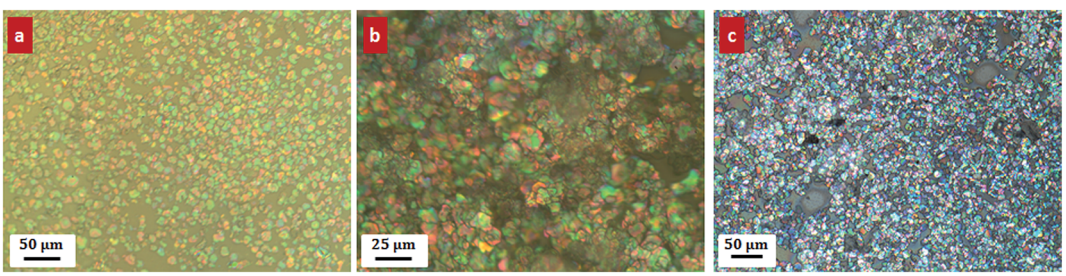

Fig. 3 Optical images of the non-optimized assemblies of the alumina tablets when: (a) there are not enough particles in the initial mixture, (b) there are too many particles in the initial mixture, (c) the concentration of catalyst is too high in the initial polymer solution.

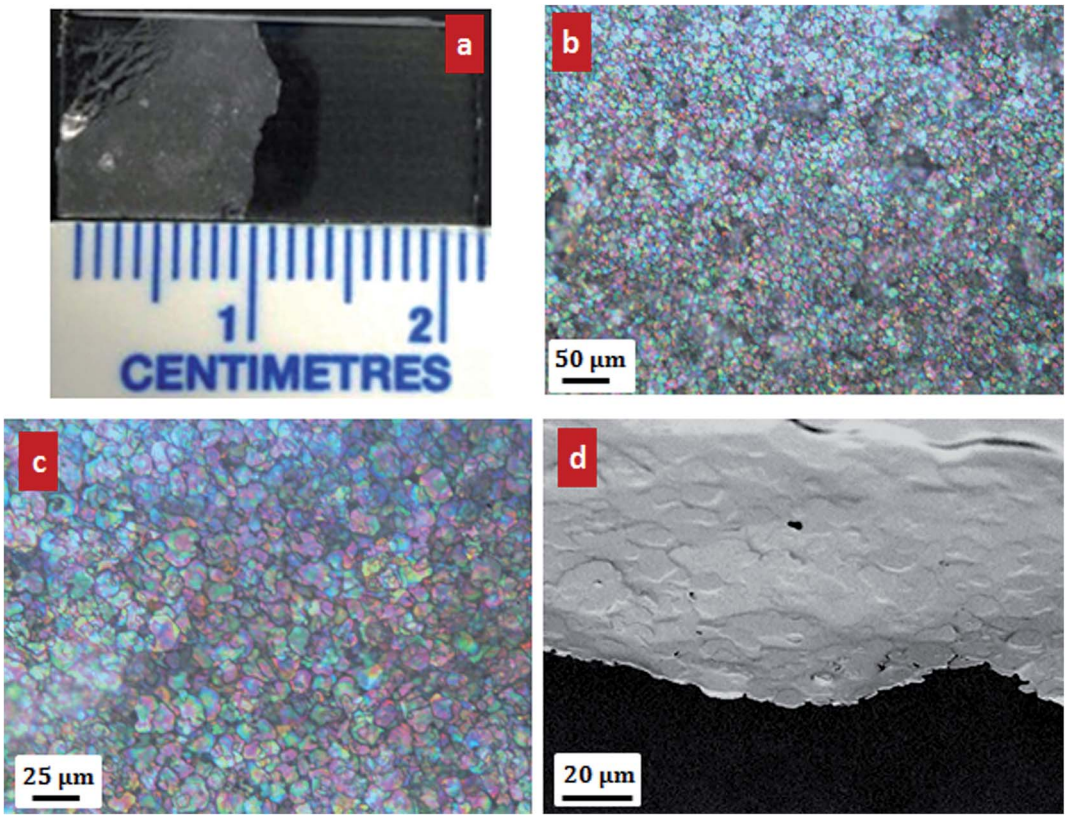

Fig. 4 Self-assembled alumina tablets embedded in a PDMS film. (a) A film on a glass slide. (b and c) Optical images of the film at two different magnifications, (d) SEM image of the film after being released from the glass slide.

(Fig. 4b and c). Upon drying, the film was sufficiently strong as to be detached from the glass slide, producing a free standing thin film of PDMS reinforced with alumina tablets (Fig. 4d).

3. Fabrication and self-assembly of micron-sized silicon tablets

The quality of the self-assembly of the alumina tablets was limited because of their irregular shape. In order to promote the self-assembly of micron-sized particles into highly periodic, space filling two dimensional patterns, we designed and fabricated precise uniform hexagonal tablets 400 nm thick and 10 μm in width. Fig. 5 details the fabrication steps for the tablets. The process started with wet oxidation of a ⟨100⟩ silicon wafer for 20 min, which created a 200 nm thick layer of SiO_2 as a sacrificial layer. A 0.4 μm thick layer of polysilicon was then coated on the oxidized wafer by way of low pressure chemical vapor deposition. The thickness of the SiO_2 and polysilicon layers was obtained using white light interferometry (Ambios XP200, CA, US).

This wafer was subsequently annealed for 30 min at 1100 °C (ref. 38) and spin-coated with a 1 μm thick layer of Shipley 1813 photoresist (Fig. 5a). The coated wafer was then soft baked at 90 °C for 60 s and was exposed to 32 mJ cm^{-2} ultraviolet light through a patterned mask with a periodic array of 10 μm wide hexagons (Fig. 5a). Developing the photoresist followed by hard baking at 115 °C for 90 s produced well defined hexagonal islands of the photoresist material (Fig. 5b). Following this step, excess polysilicon was etched by Reactive Ion Etching (RIE) in the presence of H_2 and CF_4 for 3 min, generating well-defined polysilicon hexagonal tablets (Fig. 5c). The final steps consisted of releasing the hexagonal tablets into solution. The sacrificial SiO_2 layer was partially dissolved by wet etching in a buffered 6 : 1 hydroflouric acid (HF) solution for 55 min. The duration of this step was adjusted so that on completion of etching, each hexagonal platelet was attached to the substrate by only a small pillar of SiO_2 (Fig. 5d). The wafer was then immersed in a sonication bath, which gently broke the SiO_2 pillars and released the polysilicon micro-tablets in Milli-Q water. Fig. 5e shows an image of one of the several millions of hexagonal particles produced through these steps. The hexagonal shape was successfully transferred from the mask, with only slight rounding of the corners after the lithography and etching steps. The outer shape of the silicon tablets was much more regular and more consistent than the alumina tablets described above. The size of the tablets was also large enough so that the effects of gravity prevailed over Brownian motion: polysilicon microtablets slowly sank in water and eventually sedimented at the bottom of the container.

The shape and size of the polysilicon tablets were much more uniform compared to the alumina tablets. Fig. 6 shows the comparison between the appearance and size distributions

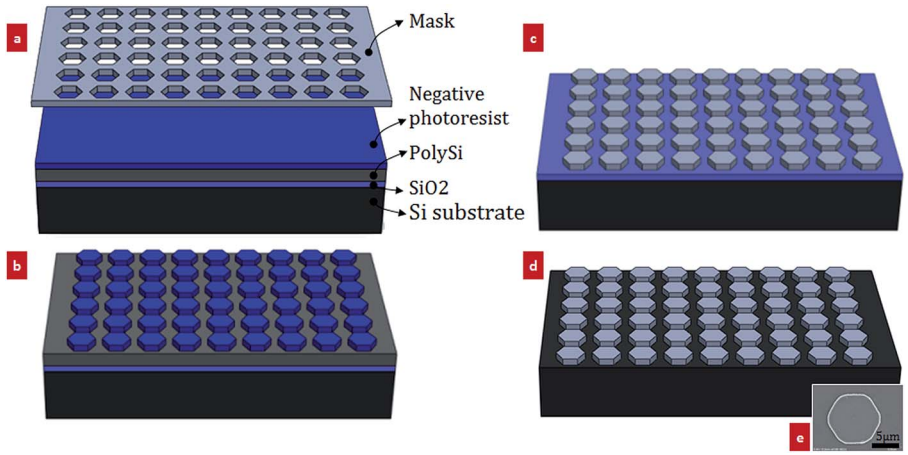

Fig. 5 Fabrication steps for the hexagonal tablets. (a) The arrangement of the layers and the mask on top. (b) The exposed photoresist is developed. (c) The excess polysilicon is etched by RIE. (d) SiO_2 is etched in HF until the tablets are only attached by a small SiO_2 pillar. (e) SEM image of a hexagonal tablet after being released in the sonication bath.

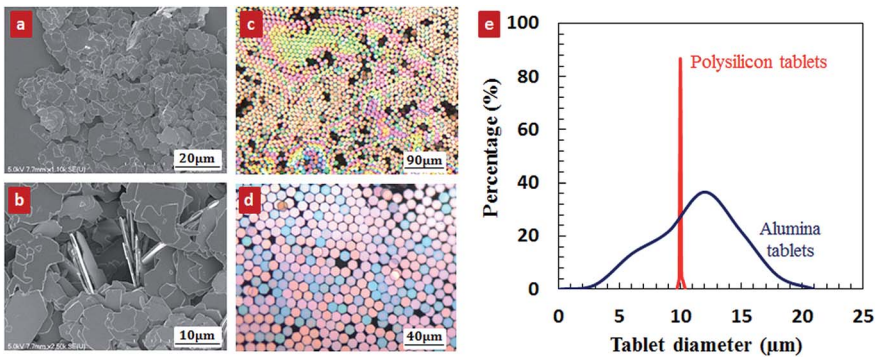

Fig. 6 The differences between the alumina and polysilicon tablets in terms of shape and size. (a and b) The SEM images of the alumina tablets used for analyzing the distribution of their size, (c and d) the optical images of the polysilicon tablets, after being assembled, used in their size analysis, (e) the frequency distribution of the size of the alumina and polysilicon tablets in percentage.

of these two types of micro-tablets. The diameter of alumina tablets was estimated by (i) calculating their surface area A obtained from analyzing their SEM images (Fig. 6a and b), and (ii) assuming that they have a circular shape. The diameter was therefore estimated as $d = \sqrt{\frac{4A}{\pi}}$. For the case of polysilicon tablets, the diameter of their circumscribed circle, obtained from analysis of their optical images (Fig. 6c and d), was considered the tablet diameter. For each case, the diameter of sixty tablets was measured and averaged. Polysilicon tablets had a highly regular size resulting in a sharp peak around 10 μm in their frequency distribution chart (Fig. 6e). The alumina tablets on the other hand were much less regular and therefore their distribution spanned over a larger range of values from ~3 μm to ~20 μm. A peak was observed around 12 μm. However, because of the slightly asymmetric shape of the frequency distribution, the average diameter was found to be less than 12 μm and instead around 10.5 μm.

The procedures described above to assemble alumina tablets were adapted to assemble polysilicon tablets into well-packed thin films. Because of their different composition, the surface of the polysilicon tablets was first coated with *n*-hexadecyltrichlorosilane ($SiCl_3(CH_2)_{15}CH_3$). The tablets were suspended in a 0.01 molar ethanol solution of the SAM for one hour at room temperature. The silane formed a hydrophobic layer covalently bonded to the surface of the tablets. The particles were then washed by repeated centrifugation/washing with ethanol (4 times) and diluted in pure ethanol to a concentration of ~4×10^5 particles per ml. The rest of the procedure followed the same steps as above. The optimized assembly conditions were also found to be the same as described for the alumina tablets. Examples of the non-optimized assemblies of the silicon tablets are shown in Fig. 7. After the assembly conditions were optimized and upon curing of PDMS, stable and well-packed self-assembled films of polysilicon particles could be collected on a glass slide (Fig. 8a). Similar to the film of alumina tablets, the film had an iridescent appearance under a microscope because of interference fringes, indicating a slight tilt of the tablets (Fig. 8b and c). However, because of the regular shape of the particles, their arrangement is much more organized. As a

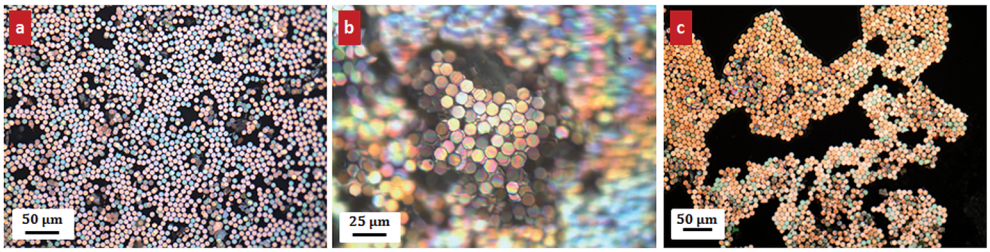

Fig. 7 Optical images of the non-optimized assemblies of the polysilicon tablets when (a) there are not enough particles in the initial mixture, (b) there are too many particles in the initial mixture, (c) the concentration of the catalyst is too high in the initial polymer solution.

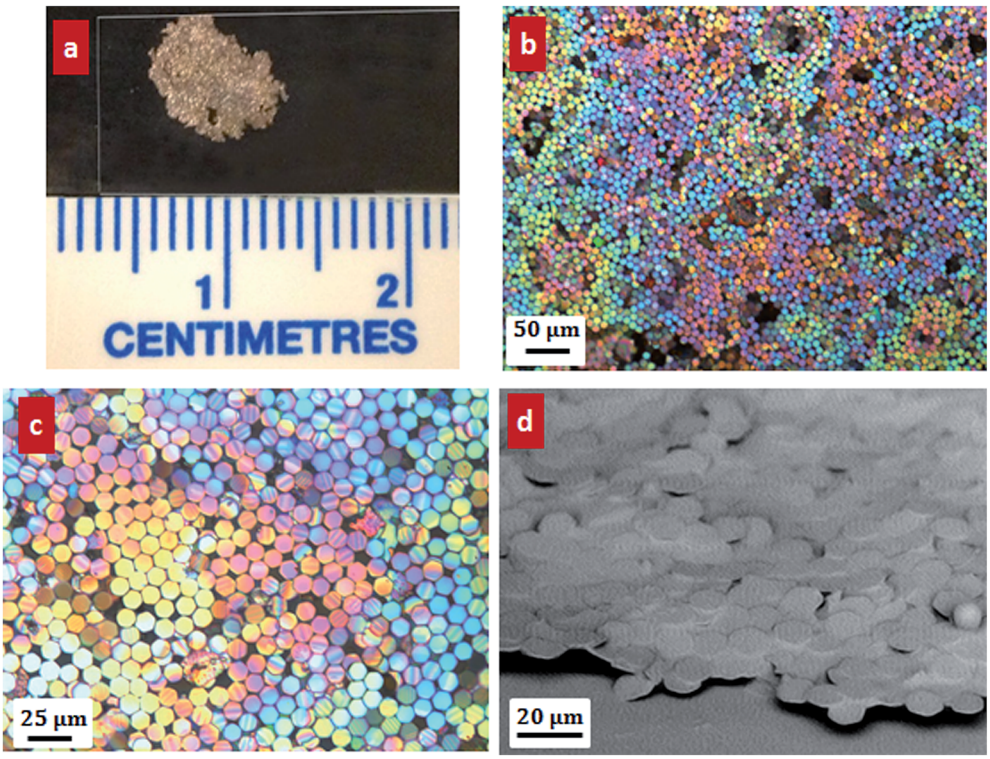

Fig. 8 Self-assembled polysilicon hexagonal tablets embedded in a PDMS film. (a) A film deposited on a glass slide. (b and c) Optical images of the self-assembled film at two different magnifications. (d) SEM image of the film after being released from the glass slide.

result, the film is optically less iridescent, largely due to the less tilt and consequently less interference fringes which form through the tablets and at their interface. Also, the films had a more packed structure, compared to the films composed of alumina tablets, resulting in a slightly higher concentration of the hard phase which is beneficial for the development of bio-inspired composites.[39] The regular structure of the films also enables a better control over the load transfer between the neighboring layers in any future multilayered materials made of these films. The self-assembled films of polysilicon tablets were also strong enough to be detached from the glass slide, producing free-standing films of particles bonded in a PDMS matrix (Fig. 8d).

The thickness of the PDMS layer on the hard particles was measured using single wavelength (633 nm) off-null-ellipsometry (Optrel Multiskop, Germany) carried out in air, and confirmed independently with nano-profilometry through a scratch with AFM. The measurements were performed on two separate preparation batches of films composed of (i) alumina tablets, and (ii) polysilicon tablets. For each batch, three separate films were prepared and the tests were performed at three locations of each film, for a total of 18 independent measurements. The results showed no significant difference between the two batches, or between samples from each batch. The thickness of the PDMS layer was found to be 60 ± 8 nm, which is almost one order of magnitude thinner than that of the hard tablets (400 nm for the polysilicon and 450 nm for the alumina tablets). Assuming a fully packed structure with no overlap or gaps between the tablets, the thickness measurements correspond to films with about 80 vol.% of hard tablets. The modulus of the PDMS layer was also obtained using Atomic Force Microscopy (AFM) indentation (Asylum Research Inc., Santa

Barbara, CA, US). A pyramidal probe with nominal tip radius of 20 nm and a spring constant of 0.12 N m^{-1} was used to indent the samples in air. The indentation depth varied from 2 to 14 nm with maximum forces ranged between 4 to 9 nN. The results were analyzed using the Johnson–Kendall–Roberts (JKR) model,[40] giving a modulus of 32 $\pm$ 3 MPa for the PDMS layer. The range of modulus for the biopolymers at the interfaces of natural nacre is 25 to 100 MPa.[41] No significant differences between the PDMS on alumina and PDMS on silicon tablets were observed. This synthesized system duplicates many of the attributes of natural nacre: nanometer thick polymeric layers on much thicker inclusions, and extremely large contrast of properties between polymer and mineral. The combination of the weak PDMS layers and high contents of hard phase (tablets) within the self-assembled films is therefore promising for future applications as bio-inspired materials.

4. Summary

The fabrication of materials with a designed microstructure at several length scales *via* smart fabrication methods such as self-assembly may find important technological application in a wide variety of fields. While self-assembly of nano-particles with dimensions in the range of 1 nm to 1 μm has been widely studied in the literature, few successful studies on the self-assembly of larger particles have been reported until now. Self-assembly of object with dimensions larger than 1 μm, however, may find various applications, for example in biomimetic materials. Previously reported self-assembled films of ~10 μm sized particles have been less stable and less organized compared to self-assembled films of nanoparticles. This study shows that large surface areas of well-packed and stable μm-sized particles can be self-assembled with the Langmuir–Blodgett technique and then secured into a PDMS thin film. PDMS was crucial to trap the relatively heavy micro-particles at the surface, and to secure them upon curing. This technique produced thin films containing ~80 vol.% tablets with a high level of organization and alignment compared to other methods reported previously. The current study opens new pathways to combinations of properties useful for a variety of applications including protective flexible but hard coatings, optical devices or adaptive membranes for filtration. In addition, the degree of alignment of the micro-tablets within the film is excellent and the mechanical properties of the polymer layers are close to those of bio-polymers found in nacre, making this method potentially attractive for the fabrication of bio-inspired materials such as synthetic nacres.

Acknowledgements

This work was supported by the Fonds de Recherche du Québec – Nature et technologies and by the Natural Sciences and Engineering Research Council of Canada. SMMV was partially supported by a McGill Engineering Doctoral Award. Antaria Limited provided the alumina tablets. The authors would also like to acknowledge Professor Sylvain Coulombe for lending his scanning electron microscope, and Jorge Lehr and Larissa Jorge for assisting with the imaging, and Béatrice Lego for assisting with the nano-indentation tests.

References

1 G. M. Whitesides and B. Grzybowski, *Science*, 2002, **295**, 2418–2421.
2 P. M. Steinert, W. W. Idler and S. B. Zimmerman, *J. Mol. Biol.*, 1976, **108**, 547–567.
3 E. R. Ballister, A. H. Lai, R. N. Zuckermann, Y. Cheng and J. D. Mougous, *Proc. Natl. Acad. Sci. U. S. A.*, 2008, **105**, 3733–3738.
4 T. D. Clark, J. Tien, D. C. Duffy, K. E. Paul and G. M. Whitesides, *J. Am. Chem. Soc.*, 2001, **123**, 7677–7682.
5 M. M. Burns, J. M. Fournier and J. A. Golovchenko, *Science*, 1990, **249**, 749–754.
6 A. Rugge and S. H. Tolbert, *Langmuir*, 2002, **18**, 7057–7065.
7 P. Poulin, H. Stark, T. C. Lubensky and D. A. Weitz, *Science*, 1997, **275**, 1770–1773.
8 A. L. Rogach, N. A. Kotov, D. S. Koktysh, J. W. Ostrander and G. A. Ragoisha, *Chem. Mater.*, 2000, **12**, 2721–2726.
9 H. H. Wickman and J. N. Korley, *Nature*, 1998, **393**, 445–447.
10 S. Mann, W. Shenton, M. Li, S. Connolly and D. Fitzmaurice, *Adv. Mater.*, 2000, **12**, 147–150.
11 A. R. Tao, J. Huang and P. Yang, *Acc. Chem. Res.*, 2008, **41**, 1662–1673.
12 H. Zeng, J. Li, J. P. Liu, Z. L. Wang and S. Sun, *Nature*, 2002, **420**, 395–398.
13 L. J. Bonderer, A. R. Studart and L. J. Gauckler, *Science*, 2008, **319**, 1069–1073.
14 T. Ming, X. Kou, H. Chen, T. Wang, H. Tam, K. Cheah, J. Chen and J. Wang, *Angew. Chem.*, 2008, **120**, 9831–9836.
15 A. Van Blaaderen, R. Ruel and P. Wiltzius, *Nature*, 1997, **385**, 321–323.
16 M. Götz, T. Fey and P. Greil, *J. Am. Ceram. Soc.*, 2012, **95**, 95–101.
17 W. Khunsin, A. Amann, G. Kocher-Oberlehner, S. G. Romanov, S. Pullteap, H. C. Seat, E. P. O'Reilly, R. Zentel and C. M. Sotomayor Torres, *Adv. Funct. Mater.*, 2012, **22**, 1812–1821.
18 I. Muševič, M. Škarabot, U. Tkalec, M. Ravnik and S. Žumer, *Science*, 2006, **313**, 954–958.
19 Z. Nie, A. Petukhova and E. Kumacheva, *Nat. Nanotechnol.*, 2009, **5**, 15–25.
20 M. Boncheva, D. A. Bruzewicz and G. M. Whitesides, *Pure Appl. Chem.*, 2003, **75**, 621–630.
21 Y. S. Lee, *Self-assembly and nanotechnology: a force balance approach*, John Wiley & Sons, New Jersey, 1st edn, 2008.
22 E. Meyer, L. Howald, R. Overney, H. Heinzelmann, J. Frommer, H.-J. Güntherodt, T. Wagner, H. Schier and S. Roth, *Nature*, 1991, **349**, 398–400.
23 P. Podsiadlo, A. K. Kaushik, E. M. Arruda, A. M. Waas, B. S. Shim, J. Xu, H. Nandivada, B. G. Pumplin, J. Lahann, A. Ramamoorthy and N. A. Kotov, *Science*, 2007, **318**, 80–83.
24 D. H. Gracias, J. Tien, T. L. Breen, C. Hsu and G. M. Whitesides, *Science*, 2000, **289**, 1170–1172.

25 R. M. Erb, R. Libanori, N. Rothfuchs and A. R. Studart, *Science*, 2012, **335**, 199–204.
26 F. Barthelat and R. Rabiei, *J. Mech. Phys. Solids*, 2011, **59**, 829–840.
27 P. Fratzl, *Curr. Opin. Colloid Interface Sci.*, 2003, **8**, 32–39.
28 C. E. Hamm, R. Merkel, O. Springer, P. Jurkojc, C. Maier, K. Prechtel and V. Smetacek, *Nature*, 2003, **421**, 841–843.
29 S. Deville, E. Saiz, R. K. Nalla and A. P. Tomsia, *Science*, 2006, **311**, 515–518.
30 F. Barthelat, *Philos. Trans. R. Soc., B*, 2007, **365**, 2907–2919.
31 A. Grinthal and J. Aizenberg, *Chem. Soc. Rev.*, 2013, **42**, 7072–7085.
32 M. Mirkhalaf, A. K. Dastjerdi and F. Barthelat, *Nat. Commun.*, 2014, **5**, 3166.
33 L. J. Bonderer, A. R. Studart, J. Woltersdorf, E. Pippel and L. J. Gauckler, *J. Mater. Res.*, 2009, **24**, 2741–2754.
34 I. C. Gebeshuber and R. M. Crawford, *Proc. Inst. Mech. Eng., Part J*, 2006, **220**, 787–796.
35 P. M. Hunger, A. E. Donius and U. G. K. Wegst, *J. Mech. Behav. Biomed. Mater.*, 2013, **19**, 87–93.
36 M. Zellner, W. Winkler, H. Hayden, M. Diestinger, M. Eliasen, B. Gesslbauer, I. Miller, M. Chang, A. Kungl and E. Roth, *Electrophoresis*, 2005, **26**, 2481–2489.
37 T. Kanai and T. Sawada, *Langmuir*, 2009, **25**, 13315–13317.
38 X. Zhang, T. Y. Zhang, M. Wong and Y. Zohar, *Sens. Actuators, A*, 1998, **64**, 109–115.
39 F. Barthelat, *J. Mech. Phys. Solids*, 2014, **73**, 22–37.
40 K. Johnson, K. Kendall and A. Roberts, *Proc. R. Soc. London, Ser. A*, 1971, **324**, 301–313.
41 A. Khayer Dastjerdi, R. Rabiei and F. Barthelat, *J. Mech. Behav. Biomed. Mater.*, 2013, **19**, 50–60.